Water-Based Peeling of Thin Hydrophobic Films

Sepideh Khodaparast, François Boulogne, Christophe Poulard, and Howard A. Stone

Phys. Rev. Lett. **119**, 154502 — Published 13 October 2017

DOI: 10.1103/PhysRevLett.119.154502

Water-based peeling of thin hydrophobic films

Sepideh Khodaparast,[1] François Boulogne,[1,2] Christophe Poulard,[2] and Howard A. Stone[1]

[1]*Department of Mechanical and Aerospace Engineering,*
Princeton University, Princeton, NJ 08544, USA
[2]*Laboratoire de Physique des Solides, CNRS, Univ. Paris-Sud,*
Université Paris-Saclay, Orsay 91400, France

(Dated: August 31, 2017)

Abstract

Inks of permanent markers and water-proof cosmetics create elastic thin films upon application on a surface. Such adhesive materials are deliberately designed to exhibit water-repellent behavior. Therefore, patterns made up of these inks become resistant to moisture and cannot be cleaned by water after drying. However, we show that sufficiently slow dipping of such elastic films, which are adhered to a substrate, into a bath of pure water allows complete removal of the hydrophobic coatings. Upon dipping, the air-water interface in the bath forms a contact line on the substrate, which exerts a capillary-induced peeling force at the edge of the hydrophobic thin film. We highlight that this capillary peeling process is more effective at lower velocities of the air-liquid interface and lower viscosities. Capillary peeling not only removes such thin films from the substrate but also transfers them flawlessly onto the air-water interface.

Water has always been a vital resource for life, not only for drinking, irrigation and industrial purposes [1], but also for its role as a natural cleaner [2]. However, recent developments in material science have lead to the invention of a large variety of water-repellent coatings [3], which are designed to feature relatively high adhesion to surfaces and resistance to moisture [4]. These features are utilized in all manners of labeling and for creation of long-lasting patterns [5]. Nevertheless, in all of these applications there are circumstances where removal of such coatings is desired, and use of solvents must be avoided either for protecting the host substrate or for environmental sustainability. Well-known examples of such thin hydrophobic film materials are the inks of permanent markers [6] and cosmetics [7] whose removal from a surface after drying requires special solvents or surfactants, which often cause damage to the substrate or irritation to the skin. In this Letter, we discuss the effectiveness of a water meniscus for removing such thin films from substrates as the meniscus slowly propagates towards the films, pins at the edge of the film and eventually peels it off the substrate.

Peeling is an ubiquitous scientific problem that occurs repeatedly in diverse classical and modern engineering applications, which often involve cleaning procedures [8], coating, manufacturing and transfer of thin films [9–12], and fabrication of three-dimensional soft elastic structures [13]. The principles of peeling have been discussed in the pioneering works of Griffith, Obreimoff and Kendall as a quasi-static propagation of an interfacial crack between the laminating substance and the host substrate [14–18]. According to the energy theory of fracture, the force required for peeling of a thin elastic film adhering to a solid substrate depends on the interfacial surface energy, the thickness and elasticity of the thin film, and the peeling angle [16, 18]. Here we introduce *capillary peeling* as an original mechanism for peeling of delicate waterproof materials.

The principle of our approach is to slowly dip a coated surface in a water bath. We observed that under certain conditions the hydrophobic film detaches from the substrate and floats at the water interface. To appreciate the basic steps of this procedure, we show snapshots of the peeling performed for marks made by Sharpie® markers in Fig. 1a (see the video in Supplemental Material SM). The ink of these permanent markers contains a terpene phenolic resin, such as SYLVARES® TP 2040 [6], which in combination with a carrier solvent and a pigment, is commonly used to promote adhesion. Similar to the marks of the permanent markers, the thin film that is created upon drying of a drop of terpene dissolved in isopropanol on a glass slide can be removed by capillary peeling (Fig. 1b). Paradoxically, the hydrophobicity of the waterproof marks, which is supposed to provide them resistance to water, allows for flawlessly detaching and transferring the materials onto the air-water interface (see the SM).

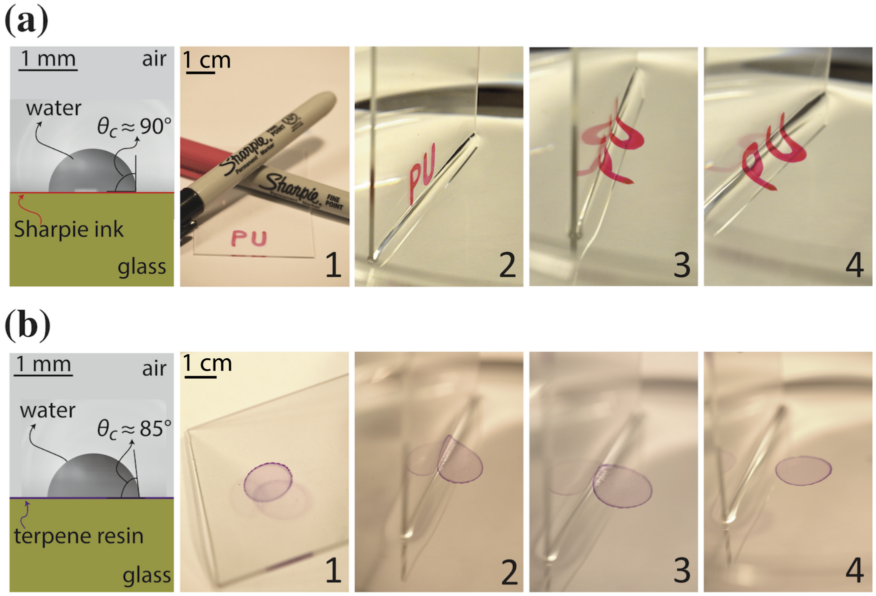

FIG. 1. Myth of the Sharpie®. (a) The letters PU, written on a glass substrate with a red permanent Sharpie® marker, are peeled off and transferred onto the air-water interface as the glass substrate is slowly dipped into a water bath. Patterns printed using Sharpie® markers on glass are otherwise resistant to rinsing with water after drying. See the movies in the SM. (b) A similar phenomenon is observed for a dried droplet of terpene phenolic resin (SYLVARES® TP 2040). For visualization, a small amount of Rhodamine B dye is added to the terpene phenolic resin. The advancing air-water interface moves at speed $U = 1$ μm/s.

To discuss the criteria for initiation and propagation of effective capillary peeling of thin films, we examine the efficiency of this method in model experiments. Indeed, as it is difficult to prepare films of terpene with uniform thickness and with annealed prestrain, we use polystyrene (PS) as a model hydrophobic material. The peeling of PS has been used for different applications by several authors, *e.g.* [19–21]. We prepared thin elastic PS films of well-controlled thicknesses $b \in [50, 1200]$ nm adhered to clean glass substrates. In all experiments, we use pure water and air as the liquid and the gas phase, respectively unless otherwise noted. We perform the experiments by keeping the vertical substrate stationary,

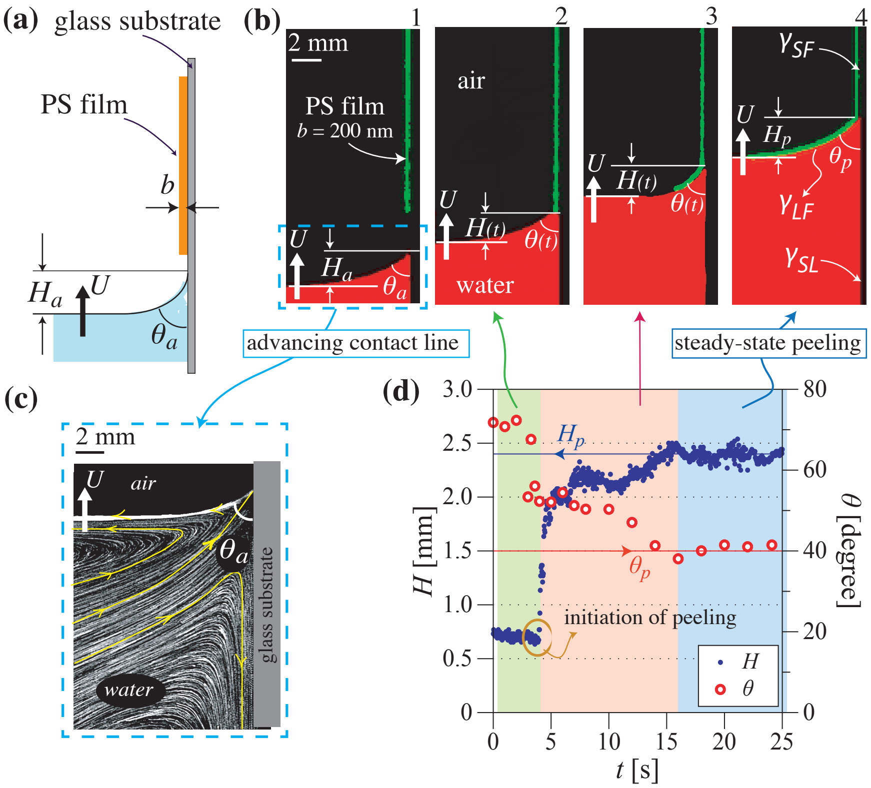

FIG. 2. Understanding capillary-driven peeling. (a) Schematic of the configuration used in the capillary peeling experiments. (b) Experimental visualizations of the main steps of the capillary peeling process. The liquid phase is labeled with a red fluorescent dye and the thin PS film ($b = 200$ nm) is covered with polystyrene microparticles to reflect the green light of the laser used in the experiments. The air-water interface moves with speed $U = 1$ μm/s on the substrate. The contact angle $\theta(t)$ changes from the advancing value θ_a on the clean substrate to the θ_p as the crack propagates in a steady-state manner. (c) On the hydrophilic glass substrate, water exhibits a split-injection flow pattern with a stagnation point at the contact point. (d) The time evolution of the experimental measurements of the height H and the angle θ of liquid wedge confirms the distinct regimes present in a successful capillary peeling process.

whilst moving the air-water interface upward using a motorized linear stage (Fig. 2a). For visualization purposes, either red fluorescent dye (Fig. 2b) or seeding tracer particles (Fig. 2c) are added to the liquid phase.

As the moving contact line reaches the edge of the thin PS film, which is adhered to the solid substrate, the surface tension applies a detachment force to the film, which drives the capillary peeling. Fig. 2b shows the main steps of a successful capillary peeling process in a vertical configuration. As the water meniscus moves upward at an average speed U, relative to the stationary substrate (Fig. 2b-1), the meniscus is pinned at the edge of the film (Fig. 2b-2). At this point the water level far from the substrate continues to rise, whilst the meniscus remains pinned at the edge. Finally, in case of successful peeling, defect-free thin films are peeled off of the vertical glass substrates and float on the free horizontal air-water interface (Fig. 2b-3,4). On a hydrophilic substrate, water exhibits a split-injection flow pattern with a stagnation point at the three-phase contact point (Fig. 2c). In this configuration, the air-liquid interface moves away from the substrate; if the contact line gets pinned when it reaches a hydrophobic film so that an interfacial crack between the film and the substrate is initiated, the flow profile guarantees that the film can be carried away from the substrate.

We show the time evolution of the height $H(t)$ and the angle $\theta(t)$ of the liquid wedge in Fig. 2d. Initially, once the contact line is pinned at the film edge, the height $H(t)$ decreases from the capillary length $\ell_c = \sqrt{\frac{\gamma}{\rho g}} \approx 3$ mm, where γ is the surface tension, ρ is the density and g is the gravitational acceleration, to a height of about 0.6 mm. When the interfacial crack between the PS film and the substrate propagates, eventually the height of the liquid wedge H and the associated macroscopic angle θ reach equilibrium values H_p (blue line in Fig. 2d) and θ_p (red line in Fig. 2d), respectively.

Therefore, three main steps compose successful capillary peeling: the advancing motion of the contact line on a clean substrate, the initiation of the crack with the meniscus pinned to the edge of the film, and the steady-state propagation of the crack (Fig. 2d). The interfacial energies of the materials, the velocity of the air-liquid interface, and the thickness of the film play crucial roles in the determining the effectiveness of the capillary peeling. Next, we discuss the effects of these three parameters, to explain the operating conditions for the initiation of the capillary peeling and the steady-state propagation of the interfacial crack when the peeling is successful.

For an ideal system without dissipation, the condition for initiating a crack between a thin elastic sheet and a smooth substrate is $G = W$, where G is the effective mechanical energy/area to separate the interfaces [18] and W is the thermodynamic work of adhesion, which is obtained from the interfacial energy balance to separate the film from the surface: the system gains the interfacial energy (per unit area) γ_{SF} between the substrate and the film but loses the interfacial energies γ_{SL} at the substrate-liquid interface and γ_{LF} at the liquid-film interface (Fig. 2b). Therefore, the thermodynamic work of adhesion is

$$W = \gamma_{SL} + \gamma_{LF} - \gamma_{SF}. \tag{1}$$

We can assess the relative importance of elastic effects on the peeling. Assuming that the beam bends similar to a thin beam fixed at the tip of the crack, the gain of energy per unit width due to the elastic bending of the film is $\mathcal{E}_B \approx \frac{Ewb^3}{12}\int_0^\ell \kappa^2 ds$, with κ and ℓ being the curvature and length of the bent section of the film, respectively. Therefore, considering the capillary length ℓ_c as the typical length scale in our geometry, the ratio of $\mathcal{E}_B$ to the gain of interfacial energy per unit width $\mathcal{E}_\gamma$ is typically on the order of $10^{-5} - 10^{-1}$ for the range of thicknesses considered in our experiments. Hence the contribution of the bending energy in Eq. (1) is neglected. The bending energy is expected to become considerable as the film thickness reaches around 10 μm in our experiments.

We use the Young-Dupré equation expressed at the tip of the peeling front to relate the contact angle observed for peeling, θ_p, to these interfacial tensions. Then, the thermodynamic work W can be expressed as [22]

$$W = \gamma_{LF}(1 - \cos\theta_p). \tag{2}$$

Using the contact angle value $\theta_p = 40°$ measured in Fig. 2, and the value for the liquid-film interfacial energy $\gamma_{LF} = 11$ mN/m determined experimentally [23], the thermodynamic work of adhesion for PS on glass is $W \approx 2.5$ mN/m. See Supplemental Material for brief description of the interfacial energy measurements.

This value can be compared to classical adhesion tests such as cleavage and blister tests with details presented in the SM, which yield $G \approx 17$ mN/m [24, 25]. The difference between G and W indicates that energy dissipation occurs and that the condition for separation should be generalized as

$$G - W = \sum_i D_i, \tag{3}$$

where D_i represent frictional, viscous or other dissipative forces (per unit length).

It is not straightforward to determine the dissipation mechanisms that occur when the triple line of the meniscus reaches the edge of the thin film, as in Fig. 1 and Fig. 2. Experimentally, we report that the success rate of the peeling depends significantly on the speed of the contact line U and also on the thickness of the film b (Fig. 3a). There are at least two paths for energy dissipation: (i) viscous dissipation due to the fluid motion and (ii) the interfacial crack propagation, which induces mechanical dissipation that is a combination of modes I and II, respectively, for the cleavage and the shear of the film [26].

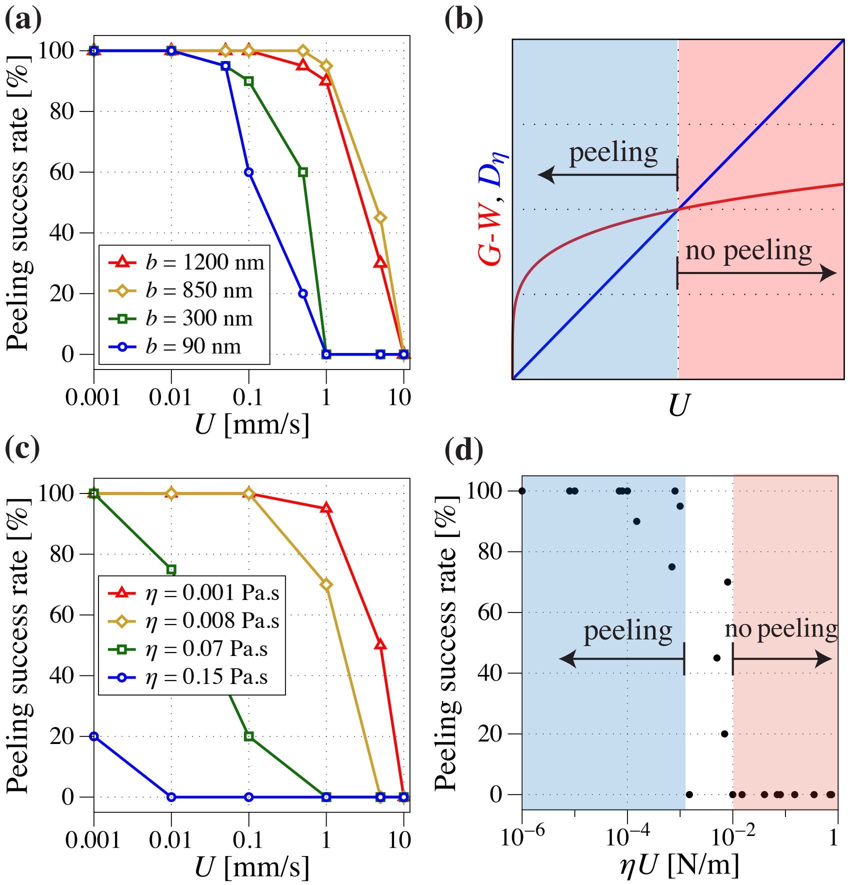

FIG. 3. Role of viscous dissipation D_η. (a) Capillary peeling becomes less efficient at higher speeds $U > 1$ mm/s, especially for very thin films $b < 100$ nm. The success rate is calculated for capillary peeling performed on 20 samples. (b) Velocity dependence of the adhesion energy G and the viscous dissipation D_η. The blue domain corresponds to an energetically favorable peeling. (c) Capillary peeling becomes less efficient at higher viscosities $\eta \approx 10^{-2}$ Pa·s for $b = 850$ nm. (d) The data from panel (c) collapse when plotted as a function of ηU. Capillary peeling tends to fail for $\eta U > 10^{-2}$ N/m.

We can compare an estimate for the viscous dissipative forces/length D_η of the liquid to pass over the film, which is proportional to ηU [27], with the adhesion energy G of the substrate-film interface. It has been observed experimentally that the velocity dependence of the adhesion energy $G(U)$ is described by a power law, $G \propto U^\alpha$ with α an exponent smaller than one, which varies typically between 0.1 and 0.4 in experimental and numerical studies

[16, 28, 29]. Therefore, if the peeling speed is greater than a critical value, the dissipated energy through viscous effects is larger than the cost of the adhesion energy (see Fig. 3b). In this case, the liquid will pass over the film and the film will not detach. In contrast, below this critical value, the capillary effects can initiate the crack. Thus, the smaller the speed of the meniscus, the higher the success rate of the peeling process for a given film thickness b, as reported in Fig. 3b. A similar trend is observed with the viscosity of the liquid: the smaller the viscosity, the higher the success rate of the capillary peeling (fig. 3c). The data for the successful capillary peeling collapse when plotted as a function of ηU and we note that the critical transition, peeling to no peeling, occurs where $\eta U/G = O(1)$ (Fig. 3d). We also recognize that for the thinnest films we have studied, e.g. typically $b < 100$ nm, defects present at the edge of the film and the substrate influence the success rate of the peeling (see SM).

Since capillary peeling is applied uniformly at the edge of the film, it allows peeling of defect-free large-area ultra thin films (Fig. 4a), which is of critical importance in fabrication of flexible and epidermal electronics [5, 9–11, 30], transparent deformable solar cells [31, 32], and flexible screens [12, 33]. Moreover, the air-water interface can serve as a platform to transfer the detached hydrophobic marks onto unconventional receiver substrates by adding a dip-coating step to the process [34] (Fig. 4b). For this purpose, first the thin film is transferred onto the air-water interface. Next, the receiver substrate, that is initially submerged vertically in the water bath, is pulled out of the bath slowly. Finally, the range of applications of capillary peeling is not limited to conventional flat substrates and provided that the criteria discussed above are met, this method can be used for peeling material from unconventional substrates of both positive and negative curvatures, following a similar procedure to that used for flat substrates (Fig. 4c).

In this Letter, we have shown that a water meniscus can effectively peel off thin elastic film from substrates to which they adhered. In a counterintuitive manner, this water-based peeling method is more effective for detachment of hydrophobic material. Providing that the capillary induced peeling force per unit length is larger than the adhesion energy per unit area of the thin film, different paths of energy dissipation may influence the effectiveness of this peeling method. Among these, we demonstrated that viscous dissipation in the advancing liquid meniscus, which scales with μU, can significantly reduce the efficiency of the capillary peeling. The fact that water naturally has high interfacial tension, relatively low viscosity

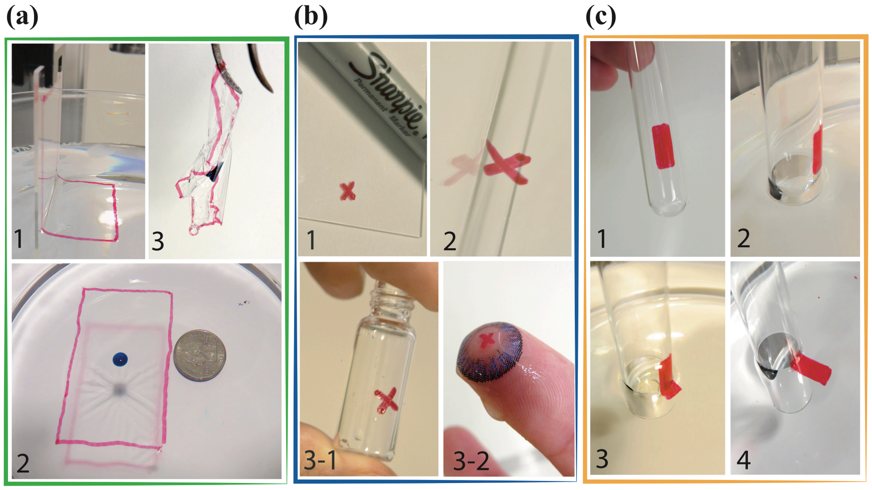

FIG. 4. Applications of capillary peeling. (a) Large-area thin films (b = 200 nm) can be (1) detached from the substrate, and (2) flawlessly transferred to the air-water interface. (3) Such thin films are otherwise difficult to handle or transferred to another substrate. (b) Complex patterns can be (1) detached from the original substrate, (2) moved onto the air-water interface and finally (3-1) and (3-2) be transferred onto unconventional substrates. Here marks made by Sharpie® pens are transferred to the curved surface of a small glass bottle (3-1) and the delicate surface of a color contact lens (3-2). (c) Water-proof thin films can be removed from unconventional curved substrates. Here the mark made by a Sharpie® pen is removed from the outer wall of a laboratory tube.

and there exists a large variety of polymers and permanent inks that are designed to be water-proof (and thus hydrophobic), makes water one of the best candidates to be used as the liquid phase in the capillary peeling method. The capillary peeling approach described here should prove applicable to a wide range of hydrophobic materials, printing techniques and emerging technologies.

ACKNOWLEDGMENTS

S.K. thanks the Swiss National Science Foundation for Early Mobility grant (P2ELP2-158896). F.B. acknowledges that part of the research leading to these results received funding from the People Programme (Marie Curie Actions) of the European Union's Seventh Framework Programme (FP7/2007-2013) under REA grant agreement 623541. H.A.S. thanks the

NSF for support via grants CBET-1509347 and DMS 1614907. We thank H. Hui for valuable discussions on the crack initiation and F. Restagno and T. Salez for discussions on the preparation of PS films.

[1] M. A. Shannon, P. W. Bohn, M. Elimelech, J. G. Georgiadis, B. J. Marinas, and A. M. Mayes, Nature **452**, 301 (2008).

[2] I. Palabiyik, M. T. Yilmaz, P. J. Fryer, P. T. Robbins, and O. S. Toker, J. Clean. Prod. **108, Part A**, 1009 (2015), ISSN 0959-6526.

[3] Y. Zhu, J. Zhang, Y. Zheng, Z. Huang, L. Feng, and L. Jiang, Adv. Funct. Mater. **16**, 568 (2006).

[4] E. Ueda and P. A. Levkin, Adv. Mater. **25**, 1234 (2013), ISSN 1521-4095.

[5] D. Kim, N. Lu, R. Ma, Y. Kim, R. Kim, S. Wang, J. Wu, S. M. Won, H. Tao, A. Islam, et al., Science **333**, 838 (2011).

[6] T. Mammen and R. Valadez, *Ink composition resistant to solvent evaporation* (2006), US Patent 7,084,191.

[7] E. J. Kim, B. J. Kong, S. S. Kwon, H. N. Jang, and S. N. Park, Int. J. Cosmetic Sci. **36**, 606 (2014).

[8] F. Boulogne and H. A. Stone, EPL **108**, 19001 (2014).

[9] Q. Cao, H. Kim, N. Pimparkar, J. P. Kulkarni, C. Wang, M. Shim, K. Roy, M. A. Alam, and J. A. Rogers, Nature **454**, 495 (2008).

[10] G. Eda, G. Fanchini, and M. Chhowalla, Nat. Nanotechnol. **3**, 270 (2008).

[11] C. H. Lee, D. R. Kim, and X. Zheng, Nano Lett. **11**, 3435 (2011), ISSN 1530-6992 (Electronic); 1530-6984 (Linking).

[12] T. Kim, K. Cho, E. K. Lee, S. J. Lee, J. Chae, J. W. Kim, D. H. Kim, J. Kwon, G. Amaratunga, S. Y. Lee, et al., Nat. Photonics **5**, 176 (2011).

[13] C. Py, P. Reverdy, L. Doppler, J. Bico, B. Roman, and C. Baroud, Phys. Rev. Lett. **98**, 156103 (2007).

[14] A. A. Griffith, Proc. Roy. Soc. Lond. A **221**, 163 (1921), ISSN 0264-3952.

[15] J. W. Obreimoff, Proc. Roy. Soc. Lond. A **127**, 290 (1930).

[16] K. Kendall, J. Phys. D Appl. Phys. **4**, 1186 (1971).

[17] K. L. Johnson, K. Kendall, and A. D. Roberts, Proc. Roy. Soc. Lond. A **324**, 301 (1971), ISSN 0080-4630.

[18] K. Kendall, J. Phys. D Appl. Phys. **8**, 1449 (1975).

[19] H. Bodiguel and C. Fretigny, Eur. Phys. J. E **19**, 185 (2006).

[20] J. Huang, M. Juszkiewicz, W. H. de Jeu, E. Cerda, T. Emrick, N. Menon, and T. P. Russell, Science **317**, 650 (2007).

[21] O. Bäumchen, J. D. McGraw, J. A. Forrest, and K. Dalnoki-Veress, Phys. Rev. Lett. **109** (2012).

[22] P. G. de Gennes, F. Brochard-Wyart, and D. Quéré, *Capillarity and Wetting Phenomena: Drops, Bubbles, Pearls, Waves* (Springer-Verlag New York, 2004), 1st ed.

[23] D. K. Owens and R. C. Wendt, J. Appl. Polym. Sci. **13**, 1741 (1969).

[24] K. Kendall, J. Adhes. Sci. Technol. **8**, 1271 (1994).

[25] F. Boulogne, S. Khodaparast, C. Poulard, and H. A. Stone, Eur. Phys. J. E **40** (2017).

[26] J. W. Hutchinson and Z. g. Suo, Adv. App. Mech. **29**, 63 (1991).

[27] E. Guyon, J. Hulin, and L. Petit, *Hydrodynamique Physique* (EDP Sciences, 2001).

[28] A. R. C. Baljon and M. O. Robbins, Science **271**, 482 (1996).

[29] M. Deruelle, L. Leger, and M. Tirrell, Macromolecules **28**, 7419 (1995).

[30] M. Kaltenbrunner, T. Sekitani, J. Reeder, T. Yokota, K. Kuribara, T. Tokuhara, M. Drack, R. Schwodiauer, I. Graz, S. Bauer-Gogonea, et al., Nature **499**, 458 (2013).

[31] T. Kim, J. Kim, C. Kang, T. E.and Lee, H. K., M. Shin, C. Wang, B. Ma, U. Jeong, T. Kim, and B. J. Kim, Nat. Commun. **6**, 8547 EP (2015).

[32] A. J. Baca, K. J. Yu, J. Xiao, S. Wang, J. Yoon, J. H. Ryu, D. Stevenson, R. G. Nuzzo, A. A. Rockett, Y. Huang, et al., Energy Environ. Sci. **3**, 208 (2010).

[33] M. Choi, Y. Kim, and C. Ha, Prog. Polym. Sci. **33**, 581 (2008).

[34] L. E. Scriven, MRS Proc. **121** (1988).